Reactivity Trends and Kinetic Inspection of Hydroxide Ion Attack and DNA Interaction on Some Pharmacologically Active Agents of Fe(II) Amino Acid Schiff Base Complexes at Different Temperatures

LAILA H. ABDEL-RAHMAN, RAFAT M. EL-KHATIB, LOBNA A. E. NASSR, AHMED M. ABU-DIEF

Chemistry Department, Faculty of Science, Sohag University, 82534 Sohag, Egypt

Received 1 February 2014; revised 24 May 2014; accepted 27 May 2014

DOI 10.1002/kin.20869
Published online 25 July 2014 in Wiley Online Library (wileyonlinelibrary.com).

ABSTRACT: The reactivity of few novel high-spin Fe(II) complexes of Schiff base ligands derived from 2-hydroxynaphthaldehyde and some variety of amino acids with the OH^- ion has been examined in an aqueous mixture at the temperature range from 10 to 40°C. Based on the kinetic investigations, the rate law and a plausible mechanism were proposed and discussed. The general rate equation was suggested as follows: rate $= k_{obs}$[complex], where $k_{obs.} = k_1 + k_2[OH^-]$. Base-catalyzed hydrolysis kinetic measurements imply pseudo–first-order doubly stage rates due the presence of mer- and fac-isomers. The observed rate constants k_{obs} are correlated with the effect of substituent R in the structure of the ligands. From the effect of temperature on the rate base hydrolysis reaction, various thermodynamic parameters were evaluated. The evaluated rate constants and activation parameters are in a good agreement with the stability constants of the investigated complexes. Moreover, the reactivity of the investigated complexes toward DNA was examined and found to be in a good agreement with the reported binding constants. © 2014 Wiley Periodicals, Inc. Int J Chem Kinet 46: 543–553, 2014

INTRODUCTION

Schiff base complexes have extensive importance as radiotracers [1], biologically active reagents [2–5],

Correspondence to: Ahmed M. Abu-Dief; e-mail: ahmed_benzoicc@yahoo.com.

catalysts for oxidation [6,7], epoxidation [8], polymerization [9], and decomposition reactions [10,11]. On the other hand, considerable attention has been paid over the past few decades in establishing substitution reactions, dissociation, hydroxide attack, and a reaction with cyanide of low-spin tris-ligand Fe(II) complexes. Some studies have been carried out on 1,10-phenanthroline complexes [12–14], complexes of substituted 2,2′–bipyridyl [15], complexes of Schiff base ligands derived from pyridine 2-carboxaldehyde [16] or 2-benzoylpyridine [17] and other derivatives [18]. Moreover, substituents effects on reactivity have been considered for base hydrolysis of tris-ligand-Fe(II) complexes of Schiff base ligands derived from 2-acetylpyridine and substituted benzylamines and their aniline analogues [19]. From a bioinorganic point of view, iron Schiff base complexes provide useful structural and electronic models for the similarly coordinated sites found in the heme iron enzymes. Moreover, these complexes are also important for the asymmetric oxidation of organic substrates, since their structure and catalytic activity are analogous with those of iron porphyrins [20]. This contribution deals with the hydroxide attack on some newly prepared and characterized Schiff base amino acid Fe(II) complexes [4]. The particular importance of the ligands used in this study (Scheme 1) is their sufficiently strong interaction

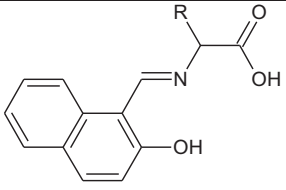

Acronym		R
Ligand	Complex	
nal	nali	CH_3
nphal	nphali	$CH_2C_6H_5$
nas	nasi	CH_2COOH
nh	nhi	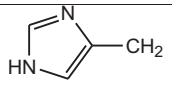
nar	nari	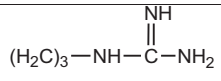

Scheme 1 Structures and abbreviations of the Schiff base ligands and abbreviations of their corresponding complexes.

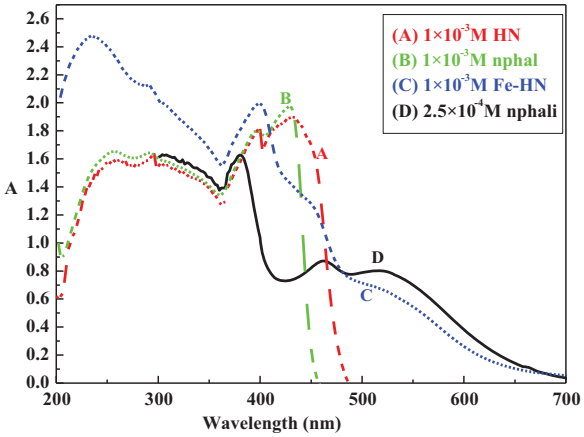

Figure 1 Molecular electronic spectra of nphali complex and its components in ethanol at 298 K.

with the Fe(II) central metal. Kinetic data concerning the base hydrolysis reaction of the important Fe(II) Schiff base amino acid complexes will help to complete the scan of pH effects on the reactivity of these vital complexes and subsequently will be very helpful in extending their applications. Substituent, temperature, and pH effects on the reactivity of these important chelates of wide applications have long been ignored, and chemists worldwide would be greatly interested in these kinetic data.

EXPERIMENTAL

Kinetic Study of the Base Hydrolysis of the Investigated Complexes

Materials and Methods. The iron(II) complexes were prepared according to the method described elsewhere [4,5,21,22]. An aqueous solution of the α-amino acid was mixed with a hot ethanolic solution of the aldehyde in stoichiometric amounts. The resulting amino acid Schiff base ligand was then stabilized by chelation to iron(II) by adding an aqueous solution of ferrous ammonium sulfate in an equivalent ratio. To avoid the Fe(II) oxidation, five to six drops of glacial acetic acid were added. The resulting solution was stirred magnetically for 9 h with continuous N_2 bubbling. The isolated complexes were recrystallized from water–ethanol solutions. The composition of the complexes was established by CHN microanalysis, IR, UV–vis spectral analyses, magnetic moment, and conductivity measurements. Full details of characterization of the present complexes can be found in our previous publications, and all gave satisfactory data [4,21]. All applied analyses are consistent with their proposal

Table I Molecular Electronic Spectra of the Prepared Schiff Base Amino Acid Fe(II) Complexes

Schiff Base Ligands and Their Complexes	λ_{max} (nm)[a]	ε_{max} (mol^{-1} cm^2)	Assignment
nali	390	3740	Intraligand band
	455	1404	LMCT band
	520 (b)	1108	d–d band
nphali	380	6520	Intraligand band
	462	3488	LMCT band
	514 (b)	3212	d–d band
nasi	380	3148	Intraligand band
	430	1113	LMCT band
	502 (b)	704	d–d band
nhi	388	3200	Intraligand band
	414 (sh), 456	2500,1746	LMCT band
	508 (b)	1380	d–d band
nari	376	2667	Intraligand band
	462	1472	LMCT band
	494 (b)	1288	d–d band

[a] b = broad, sh = shoulder.

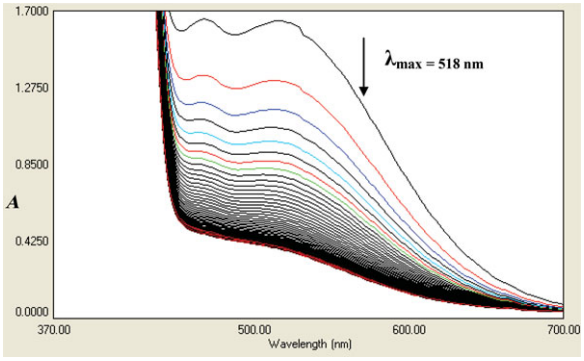

Figure 2 Repeated spectral sans of the base hydrolysis of nphali at $[OH^-] = 6.67 \times 10^{-3}$ M, $[nphali] = 1 \times 10^{-3}$ M, 514 nm, and 298 K with a time interval = 2 min.

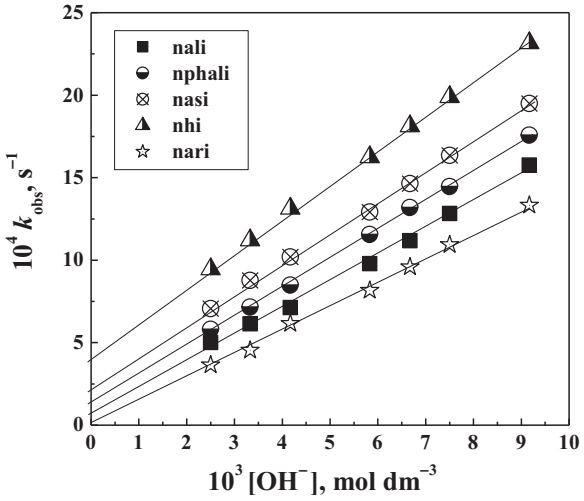

Figure 3 Plots of the observed first-order rate constant values for the base hydrolysis of investigated hydroxynaphthylidene amino acidate Fe(II) complexes as a function of $[OH^-]$ in aqueous medium at $[complex] = 1.0 \times 10^{-4}$ mol dm^{-3} and 298 K.

structures. The purity of these complexes was checked spectrophotometrically (cf. Table I), by confirming that the kinetics were exactly first order up to 90% of the reaction progress, and that the obtained rate constants agreed well with the reported values. We have tested the solutions, over a long period of time, at least a month, for the stability of the Fe(II) cation by their resistance toward reduction with dithionite. Again, if an aged complex solution was treated with NaOH under N_2, a green precipitate of $Fe(OH)_2$ was formed, indicating the presence of Fe(II) in the complex solution used in the kinetic runs. It was observed that in these runs the intense violet color of the complex solution fades during the course of each reaction. The solution then turns colorless, and some traces of green colloidal particles of $Fe(OH)_2$ turned pale yellow. Finally, the hydrolysis product was precipitated as brown $Fe(OH)_3$ by oxidation with O_2 dissolved in solution long after the end of the kinetic run.

Sodium hydroxide (99.3%), sodium nitrate (99%), and oxalic acid (99.7%) were obtained from BDH (Atlanta, GA).

Kinetic experiments were carried out by following the decrease in the absorbance at λ_{max}, the absorption maximum of the investigated complexes, in a Jasco UV–vis spectrophotometer V-530 with 10-mm matched quartz cells connected with an ultrathermostate (CRIOTERM model 190) water circulator over the first 2.5 half lives for each run [23–25]. It was confirmed that there was no interference from any other reagents at this wavelength (cf. Fig. 2 later in this article). The reactants, i.e., the complex and sodium hydroxide, were mixed so that the reaction obeyed pseudo–first-order kinetics, where $[OH^-] >> [complex]$. The pseudo–first-order constants were computed by means of a least-mean-square program from the slopes of the first-order plots

Table II Observed First-Order Rate Constant (10^4 k_{obs}, s^{-1}) values[a] for the Base Hydrolysis of Investigated Hydroxynaphthylidene Schiff Base Amino Acid Complexes in Aqueous Medium at Different [OH^-] x 10^{-3} mol dm^{-3}, [complex] = 1.0×10^{-4} mol dm^{-3}, I = 0.01 mol dm^{-3}, and 298 K

Complex [OH^-]	nali	nphali	nasi	nhi	nari
2.50	5.01	5.81	7.07	9.45	3.65
3.33	6.14	7.15	8.77	11.21	4.54
4.17	7.12	8.49	10.19	13.13	6.15
5.83	9.78	11.55	12.91	16.24	8.17
6.67	11.17	13.19	14.64	18.12	9.59
7.50	12.83	14.46	16.35	19.89	10.93
9.17	15.76	17.58	19.49	23.15	13.32

[a]The maximum error is 2%.

and are reported in Table II. The two-stage kinetics obtained from these plots was explained on the basis of the presence of the convenient labile cis and inert trans isomers of the octahedral structures [26] (cf. Fig. 4 later in this article). Standard analysis of the absorbance versus time plots gave satisfactory estimates for the slow second-stage rate constant values as reported in Table II. The concentration of sodium hydroxide was determined by using the usual analytical method with standard oxalic acid. The ionic strength of the solution was kept constant at 0.01 M using sodium nitrate. The activation parameters were calculated from Arrhenius and Eyring plots (T = 283– 313 K).

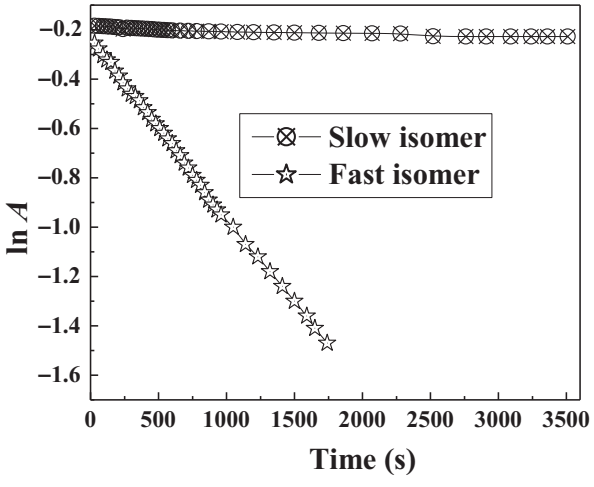

Figure 4 The observed first-order rate plots for the fast and slow isomers of nphali as worked out by Brown and Fletcher, in aqueous medium at [nphali] = 1×10^{-4} M, [NaOH] = 5.83×10^{-3} M, I = 0.01 M, and 298 K.

Kinetic Study of the Interaction of the Investigated Complexes with DNA

Calf thymus DNA, tris[hydroxymethyl]aminomethane (Tris), and EDTA were purchased from Sigma–Aldrich Chemie (Munich, Germany). The CT-DNA was dissolved in Tris–EDTA buffer (pH 7.2) and was used only for 1 day.

The interaction of the prepared complexes with calf thymus DNA was kinetically studied on a PG UV–vis spectrophotometer at 25.0 ± 1ºC.

RESULTS AND DISCUSSION

The characteristic band for the investigated complexes in the UV–vis spectra lies at λ_{max} = 494–520 nm (cf. Table I and Fig. 1). But on addition of the base, a redshift occurred. Then, this new band decays by first-order kinetics in [complex].

Repeated spectral scans (cf. Fig. 2) show first-order kinetics of the base fission of the attacked complex intermediate. The base hydrolysis reaction of the investigated complexes is simply a nucleophilic attack of the OH^- ion at the complex, which affords free ligand, and in the presence of the dissolved oxygen in the solution, colloidal Fe(III) hydroxide. The cell contents are yellow and optically clear at the end of each run. All the complexes gave evidence for two-stage kinetics. Standard analyses of the absorbance versus time traces presented good estimates for the fast and slow stages (cf. Fig. 3). It is assumed that the first stage corresponds to the parallel base hydrolysis reactivity of the more labile isomer that is expected to be fac and inert mer forms, and the second stage corresponds to the reactivity of the mer inert form only, as has been observed elsewhere [26] (cf. Schemes 2 and 3). Vichi and Krumholz reported kinetics for aquation of the iron(II) complexes derived from pyridine-2-carboxaldehyde and *n*-propylamine. They interpreted their results in terms of parallel first-order processes associated with the break of the two different iron–nitrogen bonds at sufficiently different rates of mer and fac isomers [27], which are in a thermodynamically equilibrium in solution. In the reported investigation [28], the contribution from the first step readily became smaller if a stock solution of the complex was allowed to stand for increasing periods of time because of hydrolysis of the labile isomer. In our investigated complexes, the fast isomer remains for longer periods compared with those complexes investigated elsewhere [28]

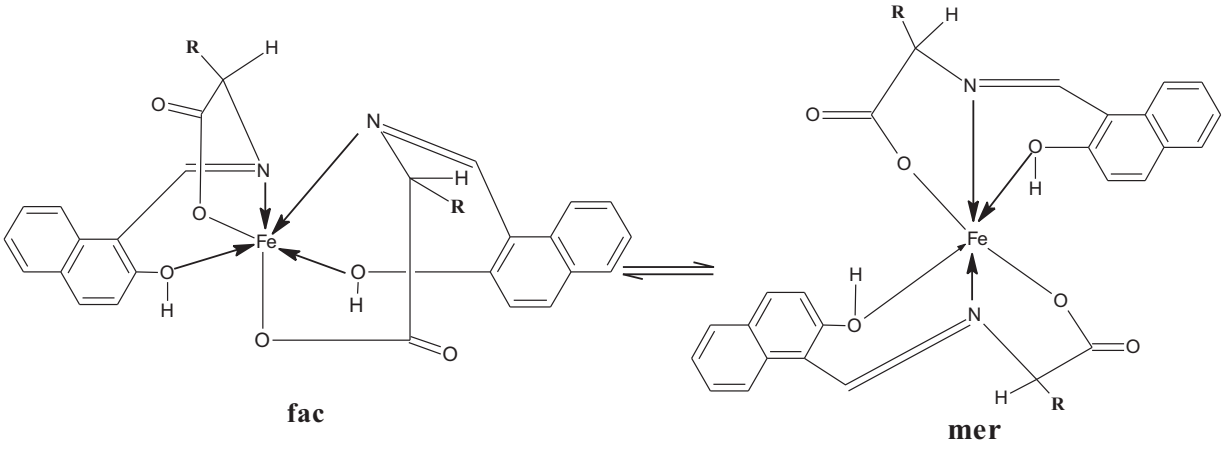

Scheme 2 Suggested isomers of nali, nphali, nasi, and nari complexes, where R is shown in Scheme 1.

Reaction Mechanism of Hydroxide Ion Attack on Iron(II) Chelates

First-order rate constants for the base hydrolysis reactions (k_{obs}) in aqueous media are cited in Table II. The plots of k_{obs} against the hydroxide ion concentration exhibited linear curves (cf. Fig. 4). The general rate law used in the case of a wide range of hydroxide concentrations and ionic strengths

$$\text{Rate} = \frac{-\text{d[complex]}}{\text{d}t} = k_1 + k_2[\text{OH}^-])[\text{complex}] \quad (1)$$

where k_1 is the rate constant of dissociation of the complex in a neutral solution. In the presence of hydroxide concentrations employed in this contribution, only the $k_2[\text{OH}^-]$ term is usually significant [29], and the observed linear k_{obs} dependences on the hydroxide ion concentration obey the following equation:

$$k_{obs} = k_1 + k_2[\text{OH}] \quad (2)$$

The values of first k_1 and second k_2 order rate constants were evaluated by least square of k_{obs} with $[\text{OH}^-]$ and are cited in Table III. It was found that the values of the observed rate constants k_{obs} are correlated with the effect of substituent R in the structure of the complexes under investigation. The order of reactivity of the prepared complexes toward the hydroxide ion attack is increased in the following sequence: nari < nali < nphali < nasi < nhi. This may be rationalized to the inductive effect of the substituent.

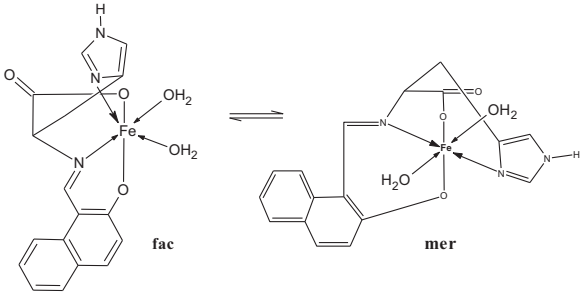

Scheme 3 Suggested isomers of the nhi complex.

The suggested mechanism for the base hydrolysis reaction of the investigated complexes is given in Scheme 4.

The proposed mechanism, for which there are precedents in ruthenium(II) chemistry [27], assumes a fast preequilibrium step in which one hydroxide ion attacks the electrophilic azomethine carbon atom [30] to form the intermediate B^{2-}. Furthermore, it is suggested that the rate-determining step implies the parallel

Table III Values of the Component Rate Constant Values[a] as Calculated by Least Squares of the Plots k_{obs} versus $[\text{OH}^-]$ of the Investigated Complexes in Aqueous Medium, at $[\text{complex}] = 1.0 \times 10^{-4}$ mol dm^{-3} and $I = 0.01$ mol dm^{-3}, and 298 K

Complex	$10^4\ k_1$	$10^2\ k_2$
nali	0.65	16.12
nphali	1.25	17.73
nasi	2.47	18.41
nhi	4.40	23.52
nari	0.013	14.61

[a] The maximum error is 2%.

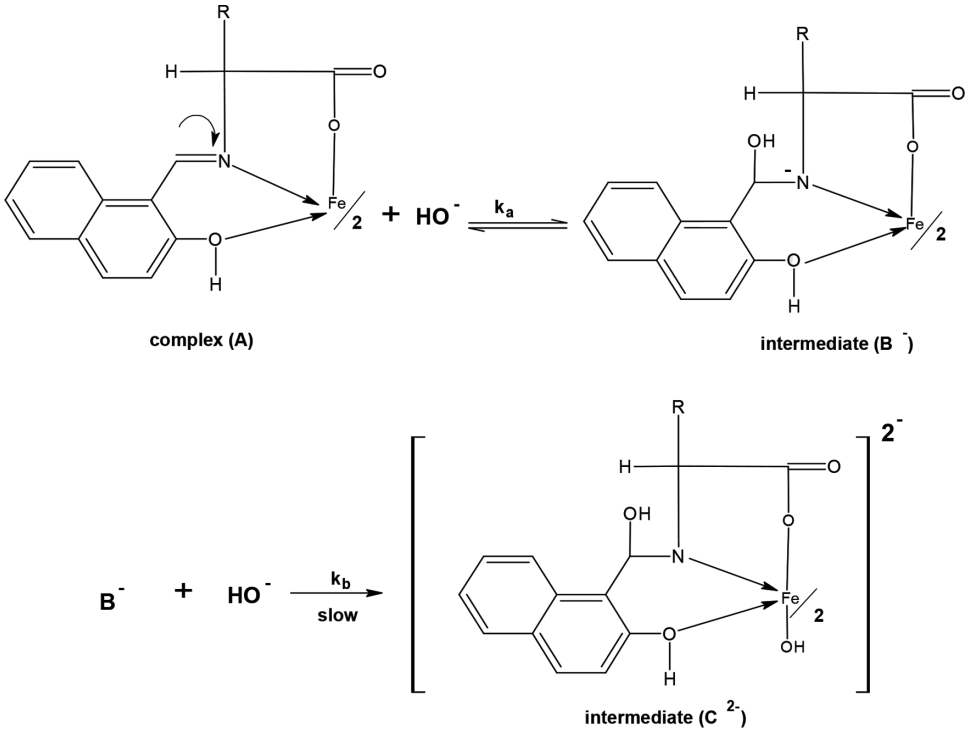

Scheme 4

attack of the hydroxide ion on the central iron atom in the intermediate B^{2-} giving the intermediate C^{3-} and the liberation of the first ligand.

Based on this mechanism, the base hydrolysis reaction rate can be derived by applying the steady-state approximation for the concentrations of the intermediates, as follows:

$$\text{Rate} = \frac{-\mathrm{d}\left[\text{complex}\right]}{\mathrm{d}t} = \frac{k_a k_b k_c [\mathrm{OH^-}][\mathrm{A}]_T}{1 + k_a k_b [\mathrm{OH^-}] + k_a k_c [\mathrm{OH^-}]} \quad (3)$$

where $[\mathrm{A}]_\mathrm{T}$ is the total analytical concentration of the complex,

$$k_{\text{obs}} = \frac{k_a k_b k_c [\mathrm{OH^-}]}{1 + k_a k_b [\mathrm{OH^-}] + k_a k_c [\mathrm{OH^-}]} \quad (4)$$

$$[A]_T = [\mathrm{A^-}]_{\text{ss}} + [\mathrm{B^-}]_{\text{ss}} + [\mathrm{C^{2-}}]_{\text{ss}} \quad (5)$$

To obtain more details about the recent reaction mechanism, the value of the reaction order (n) for $[\mathrm{OH^-}]$ was determined by a least-square procedure from the slopes of the linear plots of $\ln(k_{\text{obs}} - k_1)$ versus $\ln[\mathrm{OH^-}]$ (cf. Fig. 5), according to the following equation:

$$\ln(k_{\text{obs}} - k_1) = \ln k_2 + n \ln[\mathrm{OH^-}] \quad (6)$$

The values of n were found to be in the range from 0.759 to 1.013 for the different investigated complexes.

Figure 6 shows the dissociation curves for the studied complexes. The absorbance values of these complexes, in different aqueous buffer media, were monitored after an average time of 48 h. Thus these curves elucidate that in the solutions of pH range 4–10, the tested complexes are stable and inert against the hydroxide attack. This result is confirmed by the extremely low k_1 values, the dissociation rate constant in the aqueous neutral, and weak acidic and alkaline solutions for the investigated complexes. The maintenance of the intensely violet-colored solutions of our

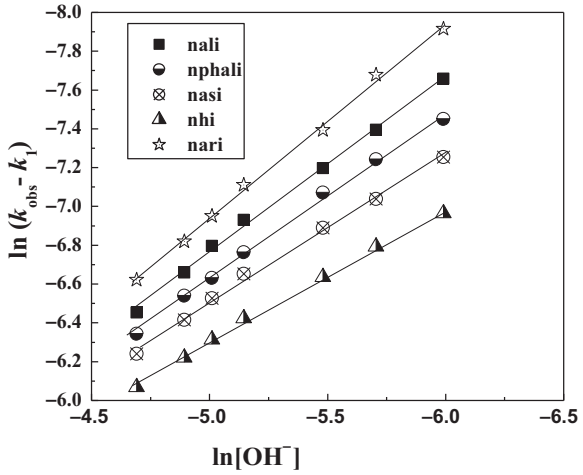

Figure 5 Plots of ln k_{obs} for the base hydrolysis of the investigated hydroxynaphthylidene amino acidate Fe(II) complexes as a function of ln[OH^-] in aqueous medium at [complex] = 1.0×10^{-4} mol $dm^{-3}$and 298 K.

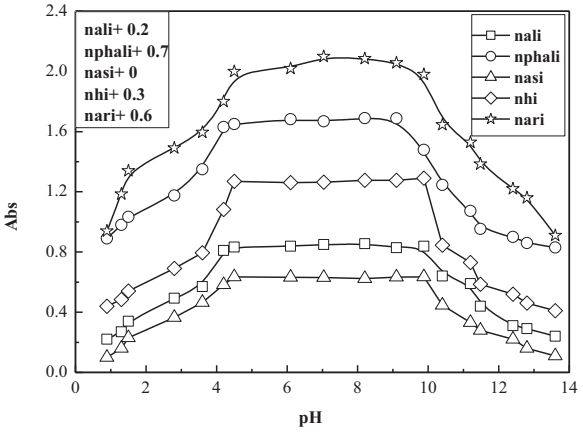

Figure 6 Dissociation curves of the prepared complexes in aqueous mixture at [complex] = 5×10^{-3} M and 298 K.

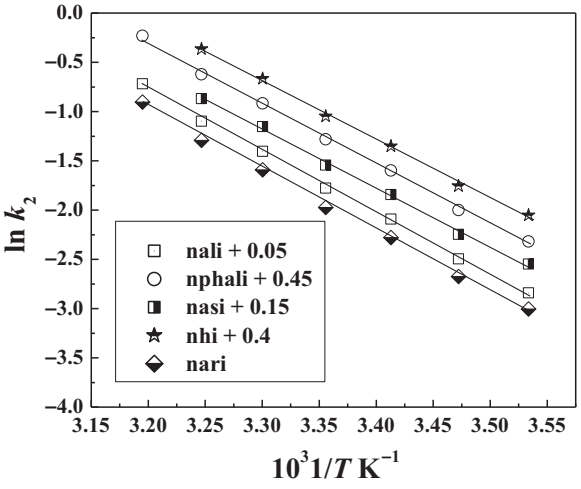

Figure 7 Plots of –ln k_2 against $1/T$ for the base hydrolysis reaction of hydroxynaphthylidene Schiff base amino acid Fe(II) complexes in aqueous medium at different temperatures.

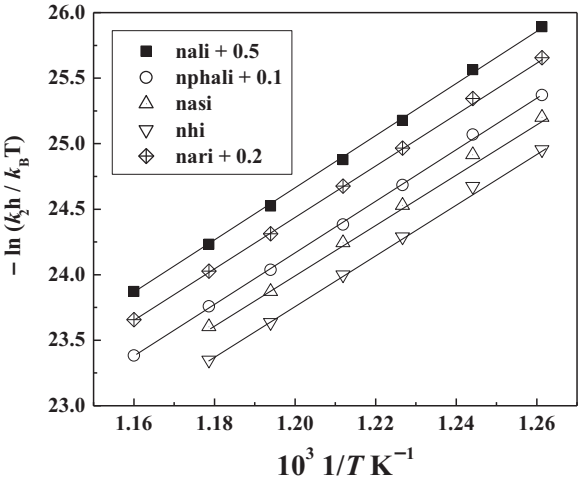

Figure 8 Plots of –(ln $k_2 h/k_B T$) against $1/T$ for the base hydrolysis reaction of hydroxynaphthylidene Schiff base amino acid Fe(II) complexes in aqueous medium at different temperatures.

complexes in the pH range 4–10 over enough average time (48 h) gives a visual appreciation of their stabilities in these solutions. This confirms the suggested mechanism since at pH > 9, the rate of base hydrolysis increases with increasing pH. The data in Table III reveal that the relative reactivity trends for our Fe(II) complexes are mainly controlled by hydrophobic and hydrophilic characters of these complexes. As hydrophobicity increases, the rate of the reaction decreases. This is ascribed to the destabilization of the more hydrophobic transient species [30] on the one hand, and the opposing stabilization of hydroxide in the aqueous media on the other hand. This explains the observed highest values of the reaction rate for nasi with much less hydrophobic character, and the lowest reported values for nari with the most hydrophobic entity.

Determination of Thermodynamic Parameters

The activation parameters for the base hydrolysis reaction were calculated, for the investigated complexes by the least-square determination of slopes and intercepts of Arrhenius and Eyring plots (cf. Figs. 7 and 8 and data collected in Table IV). It is of interest that the

Table IV Second-Order Rate Constant Values[a] $10^2\ k_2$ ($mol^{-1}\ dm^3\ s^{-1}$) and the Activation Parameters for the Base Hydrolysis Reaction of Hydroxynaphthylidene Schiff Base Amino Acid Fe(II) Complexes at Different Temperatures, [Complex] = 1×10^{-4} mol $dm^{-3}$and Ionic Strength = 0.01 mol dm^{-3} in Aqueous Medium

	Complex				
T (K)	nali	nphali	nasi	nhi	nari
283	5.56	6.27	6.73	8.61	5.21
288	7.85	8.63	9.11	11.58	7.24
293	11.75	12.91	13.64	17.34	10.76
298	16.12	17.73	18.41	23.52	14.61
303	23.34	25.49	27.18	34.43	21.38
308	31.74	34.19	36.11	46.56	28.87
313	46.42	50.63	...	...	42.58
E_a (kJ mol^{-1})	51.94	51.02	49.11	47.15	53.12
$\triangle H^{\neq}$ (kJ mol^{-1})	48.65	47.78	46.17	43.75	50.22
$\triangle G^{\neq}$ (kJ mol^{-1})	82.55	82.49	82.25	82.03	82.83
$\triangle S^{\neq}$ (J mol^{-1} K)	–113.76	–116.48	–122.11	–132.18	–109.43
A ($\times 10^7$ $mol^{-1}\ dm^3\ s^{-1}$)	9.77	8.12	5.75	1.58	13.68
pK	10.11	9.89	9.06	5.79	10.65

[a]The maximum error is 2%.

pK values calculated for the investigated complexes are in a good agreement with the kinetic and activation parameters. The higher the pK values, the stability constant of the complexes, the lower the reactivity against hydroxide ion attack and thus the greater the activation energy for the base hydrolysis reaction was observed (cf. Table IV). The pK values of the complexes were determined by the spectrophotometric continuous variation method [21]

It is worth mentioning that the activation parameters are important for the determination of the reaction rate and mechanism, From Table IV, the high negative values of the entropy of activation support the proposed mechanism that the investigated reaction takes place via the formation of an intermediate complex [24,25,31]. It is interesting that the different thermodynamic functions are consistent in their trends. As entropy of activation ($\Delta S^{\neq}$) increases, changing to less negative values, the rate constant decreases, and activation energy increases. This behavior can be ascribed to enhancing stability of activated complex intermediate.

Reactivity of the Investigated Complexes to DNA

The repeated spectral scans of the reaction between CT-DNA and the investigated complexes is characterized with formation of isosbestic points, which confirm that the reaction between them (cf. Fig. 9). The values of observed rate constants of that reaction were calculated by the least squares of absorbance with time (cf. Fig. 10 and Table V).

Table V Observed First-Order Rate Constant[a] (10^4 $k_{obs,\ s}{}^{-1}$) for the Interaction of the Prepared Complexes with CT-DNA at 298 K

Complex 10^4 [DNA]	nali	nphali	nasi	nhi	nari
2	3.24	2.55	2.81	4.15	3.65
5	4.11	3.17	3.42	5.77	4.91
8	4.78	3.8	4.13	7.11	5.85
11	5.52	4.35	4.79	8.44	6.72
14	6.16	4.87	5.32	9.83	7.65

[a]The maximum error is 2%.

Table VI Component Rate Constant Values[a] as Calculated by Least Squares of the Plots k_{obs} versus [DNA] of the Investigated Complexes in Aqueous Medium, at [complex] = 3×10^{-5} mol dm^{-3} and 298 K

Complex	$10^4\ k_1$ (s^{-1})	k_2 ($mol^{-1}\ dm^3\ s^{-1}$)	Binding Constant ($10^{-4}\ K_b\ mol^{-1}\ dm^3$)
nali	2.83	0.11	3.72 ± 0.02
nphali	2.96	0.01	2.94 ± 0.02
nasi	2.39	0.06	3.51 ± 0.02
nhi	3.31	0.56	35.73 ± 0.02
nari	3.14	0.19	6.02 ± 0.02

[a]The maximum error is 2%.

The values of observed rate constants were correlated with the reported binding constants of the interaction of the investigated Schiff base amino acid Fe(II) complexes with DNA [5]. It was found that the reactivity of the investigated complexes toward DNA is in a good agreement with the reported binding constants (cf. Table VI). The reactivity of the prepared

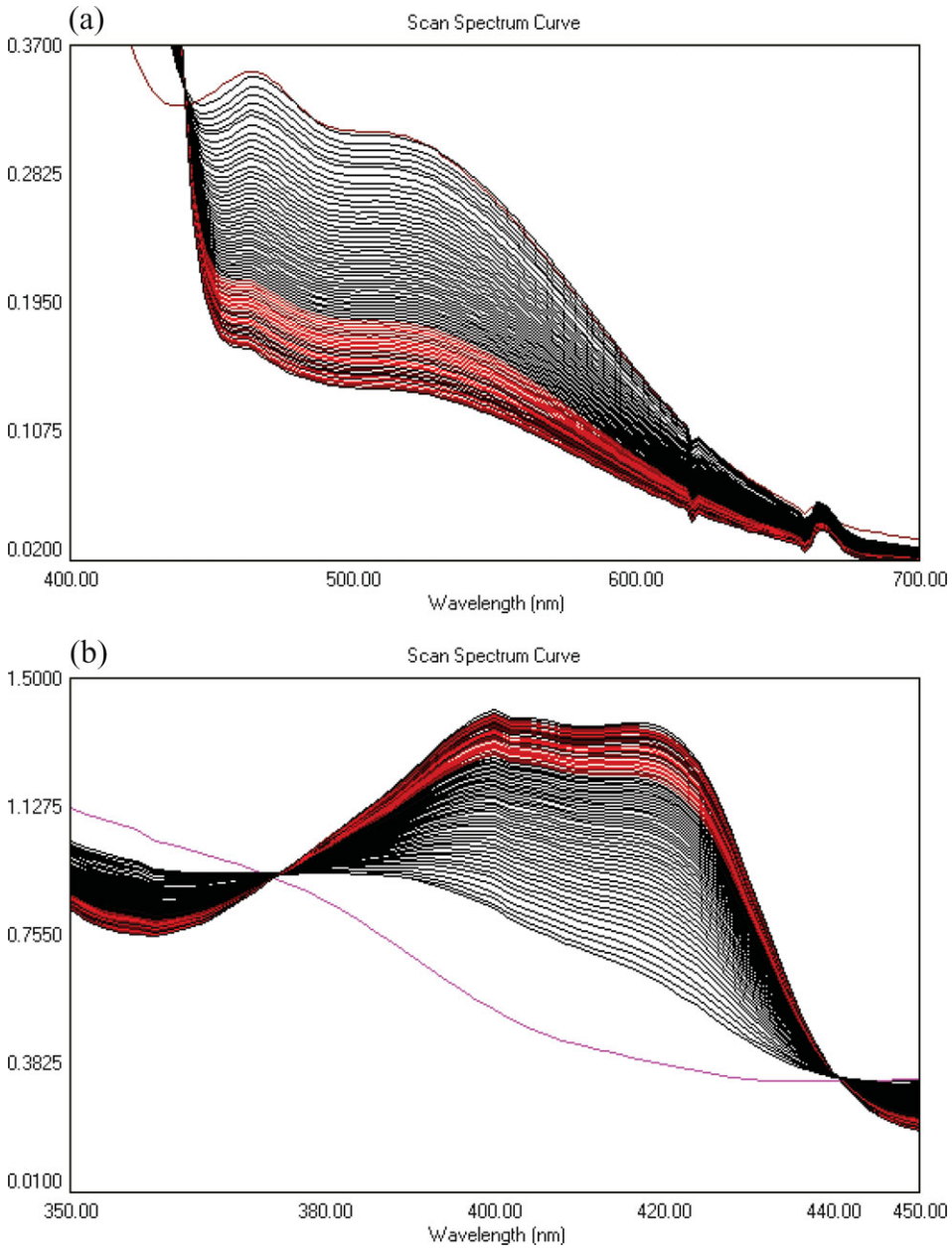

Figure 9 (a) Repeated spectral scans of nari with CT-DNA at [nari] = 1.5×10^{-3} M, [CT-DNA] = 50 μM DNA for 204 min (delay time = 4 min). (b) Repeated spectral scans of nari with CT-DNA at [nari] = 1.5×10^{-3} M, [CT-DNA] = 50 μM DNA for 204 min (delay time = 4 min).

complexes toward DNA is increasing in the following order: nphali < nasi < nali <nari < nhi.

The rate constant k_{obs} values for the interaction between CT-DNA and the investigated complexes were calculated by plotting –log *A* versus time (cf. Table V). The plot of k_{obs} versus [DNA] gave a straight line, suggesting a pseudo–first-order reaction kinetics (cf. Fig. 10).

The second-order rate constant values for the reaction between CT-DNA and the investigated complexes were calculated from the least square of k_{obs} with [DNA] and also found to be in a good agreement with binding constant values (cf. Table VI).

Linear plots of k_{obs} against [DNA] are shown in Fig. 10 and are in a good correlation with the following

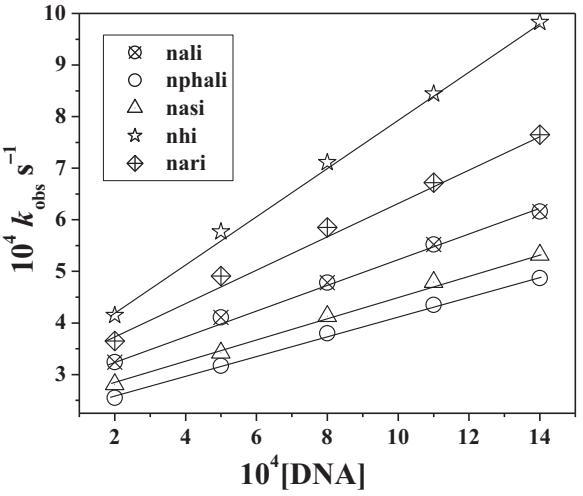

Figure 10 Plots of the observed first-order rate constant values for the interaction of the investigated Fe(II) hydroxynaphthylidene amino acidate complexes with [CT-DNA] in aqueous medium at [complex] = 3.0×10^{-5} mol dm^{-3}and 298 K.

equation:

$$\text{Rate} = -\frac{\text{d[complex]}}{\text{d}t} = k_{\text{obs}}[\text{complex}] \qquad (7)$$

The overall rate law for the investigated reaction under the adopted conditions of pseudo–first-order kinetics can be represented as follows:

$$\begin{aligned}\text{Rate} &= k_{obs}[\text{complex}] \\ &= (k_1 + k_2[\text{DNA}])[\text{complex}] \qquad (8)\end{aligned}$$

The k_1 term is assigned to the rate-determining dissociation of the investigated complexes and the k_2 term to the rate-determining attack by DNA at the compounds, where $k_{\text{obs}} = k_1 + k_2$ [DNA].

Determination of the Reaction Order

The value of the reaction order (n) for [DNA] was determined by a least-square procedure from the slops of the linear plots of ln ($k_{\text{obs}} - k_1$) versus ln [DNA] (cf. Fig. 11) according to the following equation:

$$\ln (k_{\text{obs}} - k_1) = \ln\ k_2 + n \ln [\text{DNA}] \qquad (9)$$

The values of n are recorded in Table VII. Table VII shows that the reaction between CT-DNA and the investigated complexes follows first-order kinetics in respect of [DNA].

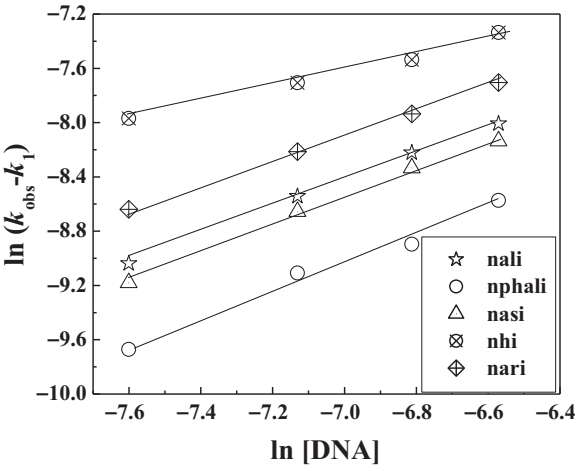

Figure 11 Plots of ln($k_{\text{obs}} - k_1$) for the base hydrolysis of the investigated Fe(II) hydroxynaphthylidene amino acidate complexes as a function of [DNA] in aqueous medium at [complex] = 3×10^{-5} mol dm^{-3}and 298 K

Table VII Reaction Order (n) Values for [DNA] as Determined by the Least Squares of the Plots ln(k_{obs}–k_1) versus ln[DNA] for the Reaction of the Investigated Complexes with CT-DNA in Aqueous Medium, at [complex] = 3×10^{-5} mol dm^{-3} and 298 K

Complex	Reaction Order (n)
nali	1.10
nphali	1.06
nasi	1.02
nhi	0.89
nari	0.90

CONCLUSION

A kinetic inspection of some high-spin Fe(II) complexes of Schiff base amino acids ligands with the OH^- ion has been examined in aqueous mixture at the temperature in the range from 10 to –40°C. The rate law and a plausible mechanism were proposed and suggested to be rate = k_{obs} [complex], where $k_{\text{obs}} = k_1 + k_2$ [OH^-]. Base-catalyzed hydrolysis kinetic measurements imply pseudo–first-order doubly stage rates due to the presence of mer- and fac-isomers. The observed rate constants k_{obs} are correlated with the effect of substituent R in the structure of the ligands. From the effect of temperature on the rate, various thermodynamic parameters have been

evaluated. The evaluated rate constants and activation parameters are in a good agreement with the stability constants of the investigated complexes. Moreover, the reactivity of the investigated complexes toward DNA was evaluated and compared with their binding constants.

BIBLIOGRAPHY

1. Luo, H.; Fanwick, P. E.; Green, M. A. Inorg Chem 1998, 37, 1127.
2. Mohamed, G. G.; Omar, M. M.; Hindy, A. M. M. Spectrochim Acta A 2005, 62, 1140.
3. El-Behery, M.; El-Twigry, H. Spectrochim Acta A 2007, 66, 28.
4. Abdel-Rahman, L. H.; El-Khatib, R. M.; Nassr, L. A. E.; Abu-Dief, A. M.; Lashin, F. E. Spectrochim Acta A 2013, 111, 266–276.
5. Abdel-Rahman, L. H.; El-Khatib, R. M.; Nassr, L. A. E.; Abu-Dief, A. M.; Ismael, M.; Seleem, A. A. Spectrochim Acta A 2014, 117, 366–378.
6. Abbo, H. S.; Titinchic, S. J. J.; Prasad, R.; Chand, S. J Mol Catal A: Chem 2005, 225, 225.
7. Gupta, K. C.; Sutar, A. K. J Mol Catal. A: Chem 2007, 272, 64.
8. Shyu, H.; Wei, H.; Lee, G.; Wang, Y. J Chem Soc, Dalton Trans 2000, 915.
9. Wu, Z.; Xu, D.; Feng, Z. Polyhedron 2001, 20, 281.
10. Nath, M.; Kamaluddin, S.; Cheema, J. Indian J Chem A 1993, 32(2), 108.
11. Gupta, K. C.; Abdulkadir, H. K.; Chand, S. J Mol Catal A: Chem 2003, 202, 253.
12. Burgess, J.; Prince, R. H. J Chem Soc 1963, 5752.
13. (a) Burgess, J. J Chem Soc (A) 1967, 431; (b) Burgess, J. Inorg Chim Acta 1971, 5, 133.
14. Burgess, J.; Prince, R. H. J Chem Soc 1965, 4697.
15. Burgess, J.; Prince, R. H. J Chem Soc 1965, 6061.
16. Burgess, J.; Prince, R. H. J Chem Soc (A) 1965, 434.
17. Burgess, J. J Chem Soc (A) 1968, 497.
18. Krumholz, P. Struct Bonding 1971, 9, 139.
19. Alshehri, S.; Burgess, J.; Shaker, A. M. Trans Met Chem 1998, 23, 689.
20. Canali, L.; Sherrington, D. C. Chem Soc Rev 1999, 28, 85.
21. Abdel-Rahman, L. H.; El-Khatib, R. M.; Nassr, L. A. E.; Abu-Dief, A. M. J Mol Struct 2013, 1040, 9–18.
22. Sharm, P. K.; Dubey, S. N. Indian J Chem A 1994, 33(12), 1113.
23. Abu-Gharib, Ezz. A.; EL-Khatib, Rafat. M.; Nassr, Lobna A. E.; Abu-Dief, Ahmed M. Z Phys Chem 2011, 225, 1.
24. Abu-Gharib, E. A.; EL-Khatib, Rafat. M.; Nassr, Lobna, A. E.; Abu-Dief, Ahmed M. J Korean Chem Soc 2011, 50(3), 346.
25. Abu-Gharib, Ezz. A.; EL-Khatib, Rafat. M.; Nassr, Lobna A. E.; Abu-Dief, Ahmed M. Kinet Catal 2012, 53(2), 182–187.
26. Blandamer, M. J.; Burgess, J.; Elvidge, D. L.; Guardado, P.; Hakin, A. W.; Prouse, L. J. S.; Radulovic, S.; Russell, D. R. Trans Met Chem 1991, 16, 82.
27. Vichi, E. J. S.; Kurmholz, P. J Chem Soc, Dalton Trans 1975, 1543.
28. Alshehri, S.; Burgess, J.; Shaker, A. M. Trans Met Chem 1998, 23, 689.
29. Blandamer, M. J.; Burgess, J.; Coohson, P.; Roberts, D. L.; Willings, P.; Mekhail, F. M.; Askalani, P. J Chem Soc, Dalton Trans 1978, 996.
30. Alshehri, S.; Blandamer, M. J.; Burgess, J.; Guardado, P.; Hurbbard, C. D. Polyhedron 1993, 12(5), 445.
31. Abu-Gharib, Ezz A.; EL-Khatib, Rafat M.; Nassr, Lobna A. E.; Abu-Dief, Ahmed M. Russ J Gen Chem 2014, 84(3), 578–585.